

INFLUENCE OF ANNEALING TEMPERATURE ON THE PROPERTIES OF ZnO SYNTHESIZED VIA 2,3-DIHYDROXYSUCCINIC ACID USING FLASH SOL-GEL METHOD

A. MODWI^{a,c}, M. A. ABBO^{b,c}, E. A. HASSAN^c, K. K. TAHA^{a,c,*}, L. KHEZAMI^a, A. HOUAS^{a, d}

^a*Al Imam Mohammad Ibn Saud Islamic University (IMSIU), College of Sciences, Department of Chemistry, Riyadh 11623, Saudi Arabia.*

^b*Taif University, College of Education and Science, Chemistry Department, Saudi Arabia.*

^c*Sudan University of Science and Technology, College of Science, Chemistry Department, , Khartoum, Sudan.*

^d*Unité de Recherche Catalyse et Matériaux pour l'Environnement et les Procédés (URCMEP); Université de Gabès; Campus Universitaire -Cité Erriadh-6072 Gabès, Tunisie.*

^e*Bahri university, College of applied & industrial sciences, Chemistry department.*

In this work, ZnO mesoporous were first time fabricated by an economic and fast sol-gel method at room temperature using 2,3-dihydroxysuccinic acid as a catalyst. The formed gel was annealed at 523, 623, 723 and 823 K for one hour. The synthesized ZnO mesoporous were characterized by different techniques. The obtained data confirmed that the prepared materials were wurtzite ZnO mesoporous with different surface area in the 109.7 to 7.48m²/g range and mean diameter of 16.03 to 25.03 nm after annealing at different temperature. Furthermore, the BET isotherms obtained were of type IV with a hysteresis type H₃, which are characteristics of a mesoporous material. The SEM micrographs revealed that the particles size increase with rise in annealing temperature. The vibration band of stretching mode of pure ZnO was shifted to lower wavenumber due to annealing from 523 to 823K.

(Received January 15, 2016; Accepted March 17, 2016)

*Keywords:*ZnO, sol-gel, 2,3-dihydroxysuccinic acid, annealing and BET surface area

1. Introduction

Recently, zinc oxide has fascinated scientists and technologist, due to its direct bandgap of 3.37 eV and large exciton binding energy of 60 meV at room temperature[1,2]. In addition to its photosensitivity, structural stability, strong oxidizing ability and non-toxicity[3,4]. These properties extend its great potential employment in photocatalysis[5], light emitting devices [6], fluorescence enhancing [7], photo – electrochemicals [8] microsensors[9]and other applications. Besides that, this semiconductor can be photoactive either under ultraviolet, visible or solar light illumination. This property is essential to promote material for the removal of chemical pollutants, existing in water. Consequently, there are great research efforts to prepare and enhance ZnO characteristics.

Several methods (physical or chemical) have been adopted to prepare the ZnO nanoparticles, such as sol-gel [10], spray pyrolysis [11], microwave irradiation [12], chemical vapor deposition [13], pulsed laser deposition [14], hydrothermal [15-17] and aqueous solution precipitation [18]. The most important and more common method to prepare nanoparticles is the sol-gel method, because of its simple and low cost [19]. In the sol-gel method, many preparation

* Corresponding author: kamaltha60@gmail.com

parameters may influence the properties of the final nanomaterials: the nature of precursors, the solvents used, the pH, the nature of the catalysts used in addition to the annealing temperature and its duration. Among all of these parameters, we looked at the last two, first time use of the 2,3-dihydroxysuccinic acid as a catalyst in the sol-gel method and studying the effect of annealing temperature.

Thus in this study, ZnO nanoparticles have been prepared by using 2,3-dihydroxysuccinic acid as a catalyst. The obtained products were annealed at four different temperatures and characterized by Brunauer–Emmett–Teller method (BET), scanning electron microscopy (SEM), X-ray diffraction analysis (XRD), Fourier transform infrared (FTIR). The effect of annealing temperature on the morphology, the chemical bonding and the surface area was studied extensively.

2. Experimental

2.1 Preparation of ZnO photocatalysts

Zinc acetate dihydrate ($\text{Zn}(\text{CH}_3\text{COO})_2 \cdot 2\text{H}_2\text{O}$), absolute methanol 99.99%, 2,3-dihydroxysuccinic acid (CHOH-COOH)₂ were purchased from Panreac and all chemicals were utilized without further purification. A certain amount of zinc acetate was dissolved in a 75 ml of methanol and stirred at 400 rpm for 30 minutes. The 2,3-dihydroxysuccinic acid catalyst was dissolved in approximately 45ml of distilled water and stirred for 30 minutes. The solution of 2,3-dihydroxysuccinic acid was added dropwise to the mixture. Under vigorous magnetic agitation a white gel was rapidly formed at room temperature and then oven dried at 358 K for 16 hours. The obtained powder was grinded prior to annealing in a tubular furnace at different temperatures ranging from 523 to 823K for one hour.

2.2 Characterization of ZnO photocatalysts

The surface area and porosity of photocatalysts were determined using a Micrometrics ASAP 2020 apparatus, (Degas temperature: ambient to 200°C⁰ for 20 minutes with pressure range from 0 to 950 mmHg). The structure, crystallinity and average particles size of photocatalysts were determined by the powder X-ray diffraction patterns, the XRD pattern of the samples were recorded by a diffractometer (D8 Advance Bruker) using Cu-K α radiation, $\lambda = 0.15406$ nm, accelerating voltage is 40kV and 20-80° as scanning angle. The morphology of the nanopowder samples was examined by a scanning electron microscope. The samples were previously oven dried at 105 °C and coated with a thin film of gold to provide ZnO powder surface with electrical conduction. The mode of chemical bonding in the prepared samples were studied by Fourier transforms infrared spectroscopy (Model: Nicolet 6700) in the range 4000 - 400 cm⁻¹ with a resolution of 4 cm⁻¹.

3. Results and discussion

3.1 Surface properties

Figs. 1 and 2 shows the nitrogen adsorption-desorption isotherms and BJH pore size distribution for pure ZnO photocatalysts annealed at the range of temperature from 523 to 823 K. All obtained isotherms, are Type IV corresponding to a capillary condensation according to IUPAC classification [20]. The hysteresis is Type H3 characteristics of a mesoporous material and did not exhibit limiting adsorption at high relative pressure (≈ 1) suggesting a slit-shaped pores. On the basis of results from figure 1, the adsorption of N₂ on ZnO photocatalysts slightly increased from low relative pressure of about 0.02 to 0.65, 0.85 and 0.95 for higher TC (623, 723 and 823 K respectively) and then followed by a sharp rise until P/P₀=1 due to substantial interparticle porosity [21]. However, for the lowest TC (523 K), N₂ adsorption is much more important and isotherm clearly increased from 0.02 to 0.4 with a large hysteresis loop indicating smaller pore size and higher surface area.

All desorption branches are different from adsorption ones indicating differences in their pore's texture [22]. Barret-Joyner-Halenda (BJH) pore size distribution for all catalysts is shown in figure.2. All plots are located in the mesoporous range, which is in agreement with the adsorption isotherm of Type IV. BJH pore size distribution of photocatalyst annealed at TC= 523 K (inset) indicates different features to that of ZnO annealed at TC= 623, 723 and 823 K, specifically from average pore diameter centered at around 9 nm. This is the result of modification in pore texture. Based on these observations, we can suggest that the annealing temperature has a clear effect on the specific surface area and the pore size distribution of the ZnO photocatalysts (Table 1, SBET decreases from 109.7 to 7.48 m²/g when TC increases from 523 to 823 K). With the increase of the annealing temperature, we notice a remarkable decrease in the surface area which can correlate to a phenomenon of a pores clogging caused by possible aggregation occurring when the annealing temperature increases.

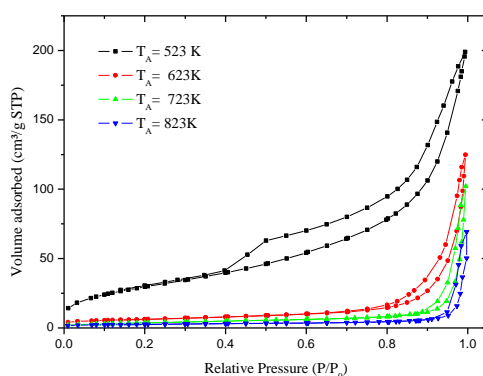


Fig.1. Nitrogen adsorption-desorption isotherms of ZnO nanoparticles annealed at different temperatures.

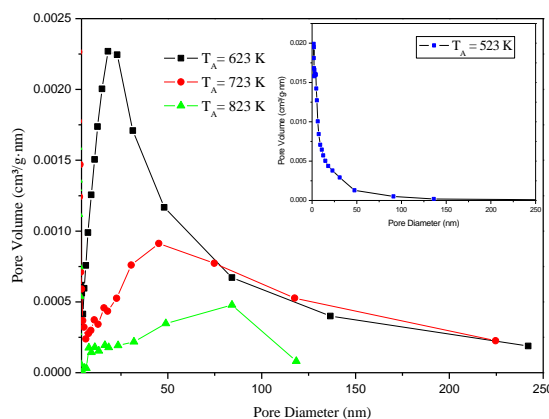


Fig.2. Barret-Joyner-Halenda (BJH) pore size distribution of ZnO nanoparticles annealed at different temperatures.

Table .1. BET surface area, pore volume and average pore diameter of ZnO nanoparticles annealed at different temperatures

Samples	BET Surface area (m ² /g)	Pore volume (cm ³ /g)	Average pore diameter (nm)
ZnO Samples			
TC= 523 K	109.7	0.313	9.96
TC= 623 K	22.13	0.194	33.53
TC= 723 K	13.21	0.158	39.8
TC= 823 K	7.48	0.053	44.03

3.2 Textural characterization by SEM

Fig.3 (a-f) shows the SEM micrographs obtained for the as prepared ZnO (a) and annealed at different temperatures (b) 523K, (c) 623 K, (d) 723 K and (f) 823K. As can be seen from the figure, the shape of the nanoparticles has changed from a plate shape of the as prepared ZnO to spherical shape after annealing. There is a little increase in the agglomeration due to the temperature increase leading to a larger particle sizes.

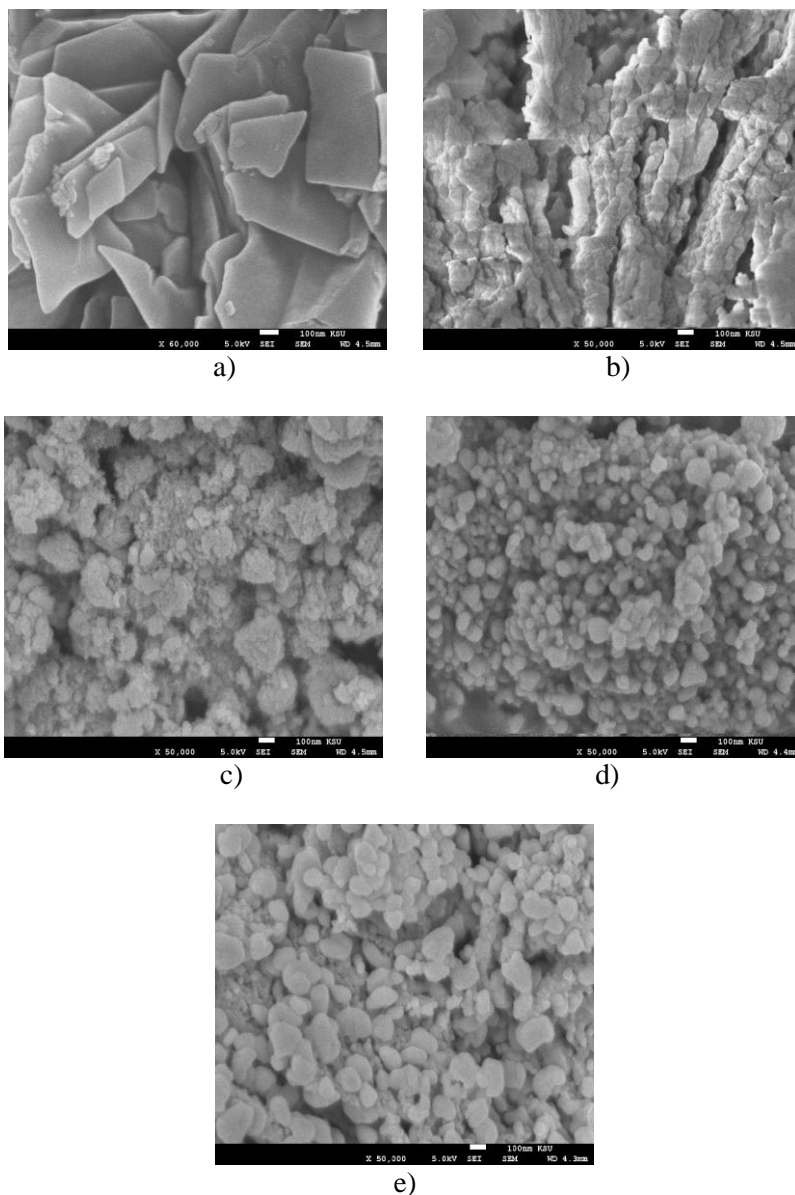


Fig..3. SEM micrographs of (a) xerogel (b) ZnO T523K (c) T623K (d) T723K and (f) 823K.

3.3 X-ray diffraction of ZnO nanoparticles

The XRD patterns for ZnO nanoparticles are displayed in (Figure.4). The results show broad peaks at position (31.61, 34.39, 36.11, 47.40, 56.52, 62.72, 66.29, 67.91 and 69.08 deg. as 2 theta). These values are in good agreement with standard card (JCPDS 36-1451) file for ZnO and can be indexed as the hexagonal wurtzite structure. The influence of annealing temperature was observed on both intensity of XRD peaks and lattice parameters. In fact, as can be seen in the (Figure.4), the principal peak (101) intensity increases with TC and the shape of this peak becomes narrower indicating an increase of the particle size. The average crystallite size (D) was calculated using the Scherrer's equation 1. [23]:

$$D = \frac{0.9 \lambda}{\beta \cos \theta} \quad (1)$$

where λ is the wavelength of Cu K α radiation, β is full width half maxima (FWHM) of the diffraction peak and θ is the Bragg peak angle. The average crystallite size and the lattice parameters of the prepared nanomaterials are presented in the Table.2. The average crystallite size of ZnO increased from 16.12 to 25.03 nm as the annealing temperature rise. These results are in good accordance with SEM micrograph and the BET measurements of specific surface area.

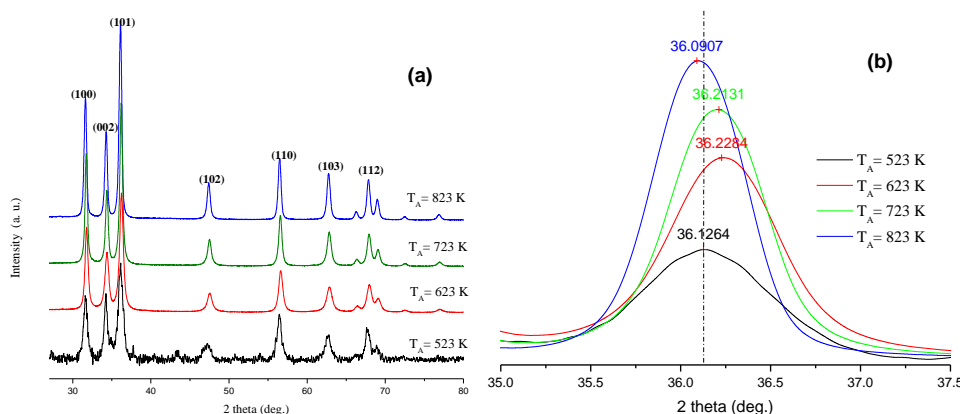


Fig.4. (a) XRD patterns of ZnO at 523, 623, 723 and 823K and (b) principal peak

Table .2. Comparison of different Specimens

Samples	2 θ (degree)	Crystallite size (nm)	Lattice parameter (\AA)		c/a
			(a)	(c)	
ZnO Samples					
TC= 523 K	36.1264	16.12	3.2732	5.2442	1.6022
TC= 623 K	36.2284	18.17	3.2608	5.2608	1.6133
TC= 723 K	36.2131	24.26	3.2491	5.2088	1.6031
TC= 823 K	36.0907	25.03	3.2628	5.2256	1.6016
JCPDS 36-1451			3.249	5.206	1.602

The d-spacing was calculated using the Bragg law:

$$d = \frac{\lambda}{2 \sin \theta} \quad (2)$$

as well as the theoretical equation :

$$\frac{1}{d_{(hkl)}^2} = \frac{4}{3} \left(\frac{h^2 + hk + k^2}{a^2} \right) + \frac{l^2}{c^2} \quad (3)$$

that relates d to the lattice constants a and c . The data obtained were almost identical (Table 3). It can also be observed that there is a decrease of inter planar spacing (d) with annealing temperature.

Table .3: The d_{hkl} for the samples annealing at different temperatures from experimental and theoretical calculations

Sample	d (Bragg)	d (theoretical)	Bond length
523K	2.4843	2.4936	1.9920
623K	2.4775	2.4881	1.9889
723K	2.4786	2.4775	1.9793
823K	2.4867	2.4856	1.9789

The Zn - O bond length L is given by[24].

$$L = \sqrt{\left(\frac{a^2}{3}\right) + \left(\frac{1}{2} - \mu\right)^2 c^2} \quad (4)$$

Where μ is the measure of an atom displacement to the neighboring one along the "c" axis. The value of μ is calculated by the equation: $\mu = \frac{a^2}{3c^2} + 0.25$. From table 3 the L values obtained are in good agreement with the 1.9749 \AA average values reported by Taha *et al.* [25].

3.4 Fourier transforms infrared studies (FTIR)

The chemical bonding and formation of xerogel, ZnO T 523K and ZnO T 823K were confirmed by FTIR measurements at room temperature. The spectra are shown in (Figure.5) and the peaks results for three samples are presented in Table 3. The broad absorption band at 3439.39 cm^{-1} and 1075.74 cm^{-1} are attributed to normal polymeric O-H stretching vibration of H_2O in the lattice of three specimens [26]. Another sharp peak 1615.60 cm^{-1} is attributed to H-O-H bending vibration, which is assigned to a small amount of H_2O in the ZnO nanocrystal [27]. The absorption band observed between 2300 and 2400 cm^{-1} are due to of the existence of CO_2 molecule in air [28]. The vibration band at 451.02 cm^{-1} is assigned to stretching mode of pure ZnO. This is shifted to lower with increase calcinations from T 523K to T 823K correspondingly. The spectrum of zinc 2,3-dihydroxysuccinate, a band at 1576.27 cm^{-1} is attributed to C=O stretching vibration of the carbonyl group in addition to strong peak at 1399.53 cm^{-1} is belong to C=O symmetric modes. The intensities at 1095 cm^{-1} , 990.19 cm^{-1} and 888.18 cm^{-1} is due to C-H vibration modes. Whereas, the small peak intensity bond at 485.60 cm^{-1} is corresponding to (O-Zn) zinc - oxygen bond [3].

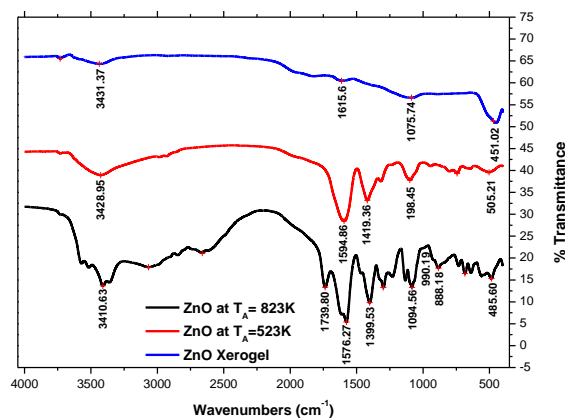


Fig.6. FTIR of ZnO xerogel, ZnO at 523K and 823K nanoparticles

Table .4. FTIR peaks and their Assignments for ZnO nanoparticles

Assignments	Wave number (cm ⁻¹)		
	ZnO xerogel	ZnO 523	ZnO 823
O-H stretching	3410.63	3426.95	3431.37
H-O-H bending vibration	1576.27	1594.85	1615.60
Zn-O stretching	485.60	504.21	451.02
C=O symmetric modes	1399.53	1419.36	-----

4. Conclusion

The ZnO nanoparticles were successfully synthesized by a sol-gel method in the presence of 2,3-dihydroxysuccinic acid as a catalyst and annealed at different temperatures. This procedure can be potentially useful for the preparation of other mesoporous catalysts with high stable yield. The N₂ adsorption-desorption isotherms of the synthesized catalysts are identified as type IV and show a type H3 hysteresis indicating the presence of mesoporous. Specific surface area decreases with the annealing temperature because of the aggregation phenomenon occurring. XRD studies confirmed the dominant presence of hexagonal wurtzite ZnO phase at lower annealing temperature with preferential orientation (101) which gradually improves with increasing the annealing temperature. The crystallite size increases from 16.12 to 25.03 nm when the annealing temperature was increased from 523 to 823K.

References

- [1] B.K. Sharma, A.K. Gupta, N. Khare, S.K. Dhawan, H.C. Gupta, *Synth. Met.* **159**, 391 (2009).
- [2] A.Olad, R.Nosrati, Preparation, characterization, and photocatalytic activity of polyaniline/ZnO nanocomposite, **323**–336 (2012).
- [3] P. Dhamodharan, R. Gobi, N. Shanmugam, N. Kannadasan, R. Poonguzhali, S.Ramya, *SpectrochimicaActa. Part A, Molecular and Biomolecular Spectroscopy*, **131**,125 (2014).
- [4] S.Sakthivel, B.Neppolian, M. V.Shankar, B.Arabindoo, M.Palanichamy, V. Murugesan, *Solar Energy Materials and Solar Cells*, 77(1), 65–82 (2003).
- [5] B. Krishnakumar, K. Selvam, R. Velmurugan, M. Swaminathan, *Desalination Water Treat.* **24**,132 (2010).
- [6] B. Krishnakumar, M. Swaminathan, *SpectrochimicaActa Part A Mol. Biomol. Spectrosc.* **81**,739 (2011).
- [7] B. Krishnakumar, M. Swaminathan, *Indian J. Chem. Sect. A-Inorganic Bio-Inorganic Phys.Theor.Anal.Chem.* **49**,1035 (2010).
- [8] C.Z. Yao, B.H. Wei, H.X. Men, H. Li, L.X. Meng, X.S. Zhang, Q.J. Gong, *J. Power Sources* **237**,295 (2013).
- [9] A. Ali, A.A. Ansari, A. Kaushik, P.R. Solanki, A. Barik, M.K. Pandey, B.D. Malhotra, *Mater.Lett.* **63**,2473 (2009).
- [10] G.Y. Shan, X.L. Xiao, X. Wang, X.G. Kong, Y.C. Liu, G. Shan, *J. Colloid Interface Sci.* **298**,172 (2006).
- [11] Y. Ni, X. Cao, G. Wu, G. Hu, Z. Yang, X. Wei, *Nanotechnology* **18**,155603 (2007).
- [12] C.R. Shabnam, P. Arun Kant, *J. Lumin.* **132**,1744 (2012).
- [13] T.H. Vlasenflin, M. Tanaka, *Solid State Commun.* **142**,292 (2007).
- [14] Y. Adachi, N. Ohashi, T. Ohnishi, T. Ohgaki, I. Sakaguchi, H. Haneda, M. Lippmaa, *J. Mater. Res.* **23**,3269 (2008).
- [15] U. Pal, P. Santiago, *J. Phys. Chem. B* **109**,15317 (2005).
- [16] H. Zhou, T.X. Fan, D. Zhang, *Microporous Mesoporous Mater.* **100**,322 (2007).
- [17] Yu, J., & Yu, X. Hydrothermal Synthesis and Photocatalytic Activity of Zinc Oxide Hollow Spheres, **42**(13), 4902(2008).

- [18] H.K. Sun, M. Luo, W.J. Weng, K. Cheng, P.Y. Du, G. Shen, G.R. Han, *Nanotechnology* **19**,125603 (2008).
- [19] J. Lee, A. J.Easteal, U. Pal, D.Bhattacharyya, *Current Applied Physics*, **9**,792 (2009).
- [20] S.J. Gregg and K.S.W. Sing, in *Adsorption, Surface Area and Porosity*, Academic Press, London, ISBN 0-12-300956-1, 1982
- [21] Xiong, G.; Luo, L.; Li, C.; Yang, X. *Energy Fuels*, **23**, 1342(2009)
- [22] Hussein, M.Z.; Al Ali, S.H.; Zainal, Z.; Hakim, M.N. *Int. J. Nanomed.*, **6**, 1373(2011)
- [23] Klug, P and Alexander, L.E. *Diffraction Procedures for Polycrystalline and Amorphous Materials*.Wiley, New York. 1954.
- [24] Barret C. S., Massalski T. B. *Structure of Metals*. Pergamon Press, Oxford (1980)
- [25] K. K. Taha, M. O. Mohamed and H. Idriss *Journal of Ovonic Research*.**11**, 271 (2015).
- [26] S. Muthukumaran , R. Gopalakrishnan, *Optical Materials*, **34**,1946 (2012).
- [27] K. Kumar, M. Chitkara, I. S. Sandhu, D. Mehta, S. Kumar, *Journal of Alloys and Compounds*, **588**,681 (2014).
- [28]K. Raja, P. S. Ramesh, D. Geetha, *SpectrochimicaActa. Part A, Molecular and Biomolecular Spectroscopy*, **131**,183 (2014).